

CQNET: CONVEX-GEOMETRIC INTERPRETATION AND CONSTRAINING NEURAL-NETWORK TRAJECTORIES

PREPRINT, COMPILED FEBRUARY 23, 2023

Bas Peters^{1*}

¹Computational Geosciences Inc.

ABSTRACT

We introduce CQnet, a neural network with origins in the CQ algorithm for solving convex split-feasibility problems and forward-backward splitting. CQnet’s trajectories are interpretable as particles that are tracking a changing constraint set via its point-to-set distance function while being elements of another constraint set at every layer. More than just a convex-geometric interpretation, CQnet accommodates learned and deterministic constraints that may be sample or data-specific and are satisfied by every layer and the output. Furthermore, the states in CQnet progress toward another constraint set at every layer. We provide proof of stability/nonexpansiveness with minimal assumptions. The combination of constraint handling and stability put forward CQnet as a candidate for various tasks where prior knowledge exists on the network states or output.

1 INTRODUCTION

The ubiquitous success of neural networks in fields like computer vision, science and engineering, and control automatically raises the desire for more intuition, control, and interpretability of its operation, as well as provable properties of the networks.

Regarding the intuition of how a trained neural network operates, classic and newer analyses for classification problems show how network layers add new decision boundaries, as viewed in terms of the input data space [1, 2, 3, 4]. A different type of intuition of how data propagates (flows) through a network (its trajectories), is provided by neural ordinary (and partial) differential equations (Neural ODEs) where the underlying continuous-time ODE, together with a discretization, prescribe (in)stability, energy conservation, invertibility similar to physical phenomena [5, 6, 7, 8, 9, 10].

Here, we propose a new network design, *CQnet*, based on the CQ algorithm [11] for the convex split-feasibility problem (SFP). The proposed network offers new insights into the operation of a network, as well as some provable properties. Specifically we

- propose CQnet and illustrate its interpretation as trajectories that are seeking feasibility with respect to a layer-dependent convex set while being elements of some other constraint sets.
- illustrate that CQnet’s most basic form naturally includes two types of (possibly data-dependent or sample-specific) constraints on the trajectories: 1) constraints that are satisfied at every layer and the output; 2) constraint sets towards which the trajectories make progress during forward propagation. CQnet can also operate with a mix of deterministic and learned constraint sets.
- require only minimal assumptions to prove the stability of CQnet in a nonexpansive sense by re-purposing ingredients from the convergence proofs of the CQ algorithm.

Besides interpreting CQnet’s inner workings, there are a few other ways to relate CQnet to existing works. Related work includes the observation that neural networks can be built from nonexpansive and averaged operators [12, 13, 14], who focus on layered networks with activation + affine structure. [15] add constraints on the network weights during the training to ensure nonexpansiveness of standard non-linear+affine composite layers, and [16, 17] construct implicit fixed point models. In this work, we prove the nonexpansiveness/stability of CQnet, or robustness to perturbations. While we also provide a layer-wise condition on the network weights, which is cheap to compute and easy to enforce, estimating entire network Lipschitz constants (see, e.g., [18, 19, 20, 13, 21]) is not the scope of this work.

Another line of work concerns neural networks with various types of state constraints. Satisfying constraints on the output of a network is possible either via the projection of the output of the last layer [22], or by training the network such that the output satisfies certain properties, for instance via alternating optimization schemes [23, 24, 25, 26], penalties added to the loss [27, 28], Lagrange multipliers [29, 30], or by training the network via a feasibility problem [31, 32]. Optimizing a network to satisfy constraints does not provide strict guarantees that validation samples will satisfy those constraints, particularly for very small datasets. For this reason, [33] propose a method for sample-specific constraints, and [34] present an approach for constraining trajectories and outputs based on differential-algebraic equations.

Furthermore, while the proposed CQnet is part of the family of deep unrolled existing algorithms, e.g., [35, 36, 37, 38], the overall goal is *not* unrolling yet-another-algorithm to hopefully obtain (minor) computational advantages or image reconstruction improvements. Instead, we focus on the interpretation, the multiple ways to employ CQnet for constraining trajectories, and a few provable properties.

The paper proceeds by reviewing the CQ algorithm and a version of its convergence proof. This sets the stage to introduce the main contribution: CQnet and a corresponding proof of stabil-

arXiv:2302.10895v1 [cs.LG] 9 Feb 2023

ity, as well as some variations and connections to other neural network types. Examples in small and large data classification and optimal control illustrate a couple of ways how CQnet can be employed while highlighting a combination of capabilities that most other networks cannot offer.

2 PRELIMINARIES AND THE CQ ALGORITHM FOR CONVEX SPLIT-FEASIBILITY

A subset of convex optimization problems may be conveniently formulated as the convex split-feasibility problem (SFP) [39, 40]

$$\text{find } \mathbf{x} \text{ s.t. } \mathbf{Ax} \in Q \text{ and } \mathbf{x} \in C, \quad (1)$$

where $\mathbf{x} \in \mathbb{R}^n$ are the optimization variables, $\mathbf{A} \in \mathbb{R}^{m \times n}$ is a matrix, and Q and C are closed and convex sets.

While there are many ways to solve the SFP, the CQ algorithm [11] offers an approach that avoids matrix inverses of \mathbf{A} and breaks down potentially difficult-to-compute projections into ‘simple’ projections and matrix-vector products. The method minimizes over the set C the objective function

$$f(\mathbf{x}) = \min_{\mathbf{x} \in C} \frac{1}{2} \|P_Q(\mathbf{Ax}) - \mathbf{Ax}\|_2^2, \quad (2)$$

where P_Q is the Euclidean projection from \mathbb{R}^n onto the closed and convex set Q , i.e.,

$$P_Q(\mathbf{x}) = \arg \min_{\mathbf{y}} \frac{1}{2} \|\mathbf{y} - \mathbf{x}\|_2^2 \text{ s.t. } \mathbf{y} \in Q. \quad (3)$$

The objective $f(\mathbf{x})$ is the squared Euclidian distance from \mathbf{x} to the constraint set $\{\mathbf{x} \mid \mathbf{Ax} \in Q\}$ restricted to C . The continuously differentiable (squared) distance function $d^2(\mathbf{y}) : \mathbb{R}^n \rightarrow \mathbb{R}$

$$d^2(\mathbf{y}) = \frac{1}{2} \|P_Q(\mathbf{Ay}) - \mathbf{Ay}\|_2^2, \quad (4)$$

has a closed-form gradient [41, Ex. 3.3]

$$\nabla_{\mathbf{y}} d^2(\mathbf{y}) = \mathbf{A}^\top (\text{Id} - P_Q) \mathbf{Ay}, \quad (5)$$

with Id as the identity operator. Lipschitz continuity with parameter λ for any $\mathbf{x} \in \mathbb{R}^n$ and $\mathbf{y} \in \mathbb{R}^n$ implies

$$\|f(\mathbf{x}) - f(\mathbf{y})\|_2 \leq \lambda \|\mathbf{x} - \mathbf{y}\|_2, \quad (6)$$

and is called nonexpansive if $\lambda \leq 1$, contractive if $\lambda < 1$. For the squared distance function (4) including linear operators \mathbf{A} , we have $\lambda = \rho(\mathbf{A}^\top \mathbf{A})$ as the largest eigenvalue [42, Lemma 8.1].

An operator T is α -averaged if it can be written as the sum of the identity operator Id and a nonexpansive operator V ,

$$T = \alpha \text{Id} + (1 - \alpha)V, \quad (7)$$

for $\alpha \in (0, 1)$. The CQ algorithm finds a solution to (1) by performing projected-gradient descent with stepsize $\alpha \in (0, 2/\lambda)$ on the distance function, resulting in the iteration

$$\mathbf{x}_{k+1} = P_C(\mathbf{x}_k - \alpha \mathbf{A}^\top (\text{Id} - P_Q) \mathbf{Ax}_k), \quad (8)$$

This shows that \mathbf{x}_k is always feasible with respect to C , and descends towards the constraint set $\{\mathbf{x} \mid \mathbf{Ax} \in Q\}$.

The CQ algorithm found uses in many applications, including radiation therapy treatment planning [43, 44], compressed sensing [45, 46], Gene regulatory network inference [47], image

deblurring [48], and adding constraints to the output of neural networks [32].

The convergence of the CQ algorithm (e.g., [42]) and its connection to forward-backward splitting [49] is the cornerstone of several properties of the neural network proposed in this work. Here, we state a version of the proof so that elements will be reused in our theorem in a later section.

Theorem 2.1 (Convergence of the CQ iteration). *If $X = C \cap \{\mathbf{x} \mid \mathbf{Ax} \in Q\} \neq \emptyset$, let λ be the largest eigenvalue of $\mathbf{A}^\top \mathbf{A}$, and $\alpha \in (0, 2/\lambda)$, then from any initial guess the iteration (8) converges to a solution in the sense that at iteration k we have $\inf_{\mathbf{y} \in X} \|\mathbf{y} - \mathbf{x}_k\|_2 \rightarrow 0$ monotonically non-increasing.*

Proof. Rewrite the CQ iteration (8) as the fixed point iteration $\mathbf{x}_{k+1} = P_C(\mathbf{x}_k - \alpha \mathbf{A}^\top (\text{Id} - P_Q) \mathbf{Ax}_k) \leftrightarrow \mathbf{x}_{k+1} = T(\mathbf{x}_k)$. According to Krasnosel’skiĭ–Mann [50, 51] (see also, e.g., [52, Thm. 1]), this iteration converges to a fixed point of T if it is an averaged operator.

To show this, write as a composition $T = P_C(I - \alpha B)$, where the projection operator P_C is nonexpansive and averaged [53, Sect. 3.1], and $B = \nabla_{\mathbf{y}} d^2(\mathbf{y})$ as in (5) is λ -Lipschitz continuous. Therefore, $(I - \alpha B)$ [53, Sect. 5] is averaged for $\alpha \in (0, 2/\lambda)$. The composition T is thus averaged, see, e.g., [52, Thm. 27]. \square

3 CQNET

The goal is to construct a neural network that offers a clear interpretation of its inner workings in terms of convex geometry. Its foundation in constrained optimization equips the proposed network with constraints on the state trajectories and output.

We modify the CQ algorithm into a neural network by making the matrix \mathbf{A} iteration dependent (\mathbf{A}_k) and learnable; network states \mathbf{x}_k are not learnable; initial guess \mathbf{x}_1 corresponds to the input data \mathbf{d} . Each CQ iteration is equivalent to a layer in the neural network. The last important item is that the projection operators P_{C_k} and P_{Q_k} are now layer dependent (not learnable in this work) and function similarly to an activation function. For instance, the widely used ReLU activation $\text{ReLU}(\mathbf{x}) = \max(\mathbf{x}, 0)$ is equivalent to the projection onto the set of elementwise bound constraints $\{\mathbf{x} \mid \mathbf{x} \geq 0\}$. The CQnet with f layers thus takes the form

$$\mathbf{x}_{k+1} = P_{C_k}(\mathbf{x}_k - \alpha \mathbf{A}_k^\top (\text{Id} - P_{Q_k}) \mathbf{A}_k \mathbf{x}_k) \quad (9)$$

for $k = 1, 2, \dots, f$ and $\mathbf{x}_1 = \mathbf{d}$

At every layer, CQnet’s states \mathbf{x}_k take a step toward the constraint set $\{\mathbf{x} \mid \mathbf{A}_k \mathbf{x} \in Q_k\}$, which changes at every iteration. In other words, the network states follow the learnable constraint set and stop moving whenever they become elements of the set. Furthermore, the states are always feasible with respect to the set C_k . Note that if we would allow for a slight generalization of the CQ algorithm and look at proximal maps instead of just projections, a larger number of common activation functions [12, sect. 2.1] fit in the proposed framework.

3.1 Stability

To prove the stability of CQnet, we borrow from the convergence of the CQ algorithm (Theorem 2.1).

Theorem 3.1 (Stability of the forward propagation of CQnet (9)). *Let $g(\{\alpha_k\}, \{\mathbf{A}_k\}, \mathbf{d})$ describe the forward propagation of data \mathbf{d} through CQnet (9) with learned weights $\{\mathbf{A}_k\}$ for $i = 1, 2, \dots, f$ layers with stepsizes $\alpha_k \in (0, 2/\lambda_k) \forall k$ and $\lambda_k = \rho(\mathbf{A}_k^\top \mathbf{A}_k)$ is the largest eigenvalue of $\mathbf{A}_k^\top \mathbf{A}_k$. Then CQnet is stable in the nonexpansive sense $\|g(\{\alpha_k\}, \{\mathbf{A}_k\}, \mathbf{d}_1) - g(\{\alpha_k\}, \{\mathbf{A}_k\}, \mathbf{d}_2)\| \leq \|\mathbf{d}_1 - \mathbf{d}_2\|$.*

Proof. Write a single CQnet layer $\mathbf{x}_{k+1} = P_{C_k}(\mathbf{x}_k - \alpha_k \mathbf{A}_k^\top (\text{Id} - P_{Q_k})(\mathbf{A}_k \mathbf{x}_k)) \leftrightarrow \mathbf{x}_{k+1} = T(\mathbf{x}_k)$ as a fixed-point iteration. Forward propagation then amounts to a composition of f operators $T_f \cdots T_2 T_1 \mathbf{d}_1 = g(\{\alpha_k\}, \{\mathbf{A}_k\}, \mathbf{d}_1)$.

Compose each operator as $T_k = P_{C_k}(\text{Id} - \alpha_k B_k)$, where the projection operator P_{C_k} is nonexpansive (and averaged) (e.g., [53, Sect. 3.1]) and $B_k = \nabla_y d^2(y, \mathbf{A}_k)$ as in (5) is λ_k -Lipschitz continuous with $\lambda_k = \rho(\mathbf{A}_k^\top \mathbf{A}_k)$ as the largest eigenvalue [42, Lemma 8.1]. Therefore, $(\text{Id} - \alpha_k B_k)$ has the Lipschitz constant $\max(1, |1 - \alpha_k \lambda_k|)$. Nonexpansiveness of $(\text{Id} - \alpha_k B_k)$ follows directly for $\alpha_k \in (0, 2/\lambda_k]$.

The product of the two nonexpansive operators $T_k = P_{C_k}(\text{Id} - \alpha_k B_k)$ is also nonexpansive. By induction, the product of f nonexpansive operators is again nonexpansive and we obtain $\|T_f \cdots T_2 T_1 \mathbf{d}_1 - T_f \cdots T_2 T_1 \mathbf{d}_2\|_2 \leq \|\mathbf{d}_1 - \mathbf{d}_2\|$. \square

The above proof is quite flexible in the sense that there are no assumptions like constant or ‘slowly’ varying network weights, as sometimes found in continuous-time ODE-based stability proofs. The proof also includes state/layer normalization, as will be shown in section 3.6 below. Theorem 3.1 also allows for different projections/activations per layer. In the next section, we take a closer look at the relation between α_k and \mathbf{A}_k .

3.2 Practical certificate of nonexpansiveness

Theorem 3.1 ensures stability (nonexpansiveness) of the network for sufficiently small α_k , given \mathbf{A}_k . In practice, however, we may desire guarantees that the network is nonexpansive during and after training, for a fixed α_k .

Our starting point is that we need an upper bound on the largest eigenvalue $\lambda_k = \rho(\mathbf{A}_k^\top \mathbf{A}_k)$. For small matrices \mathbf{A}_k we can directly compute the largest eigenvalue. The more challenging case is when convolutional kernels parameterize \mathbf{A} with multiple input and output channels. [54] present a method to compute the eigenvalues in this case, based on FFTs and SVDs, and its computational cost depends on n^2 , making the computation expensive for large-scale inputs. To proceed with deriving an upper bound on the eigenvalues that is in closed form, non-asymptotic, and independent of n , we leverage work on stepsize selection for the CQ algorithm, see, e.g., [11, 55, 56, 57, 58, 45, 48]. Although those works aim for stepsizes that accelerate convergence or avoid matrix inverses and eigenvalue computations, we repurpose the results to obtain a certificate of nonexpansiveness of CQnet (Proposition 3.2) with very little (computational) effort.

[11] presented a bound for dense and sparse matrices. Below we specialize that bound to matrices where each block is a different Toeplitz matrix generated by a convolutional kernel (the blocks on a diagonal are not the same).

Proposition 3.2 (Upper bound on the largest eigenvalue of $\mathbf{A}(\Theta)^\top \mathbf{A}(\Theta)$). *Let $\mathbf{A}(\Theta)$ be a matrix with $c_{\text{out}} \times c_{\text{in}}$ Toeplitz*

structured blocks, where c_{out} and c_{in} are the number of output and input channels respectively. Each block is parameterized by a different convolutional kernel $\theta^{i,j} \in \mathbb{R}^{w \times w}$ with w^2 elements. Also assume that the convolutional kernels are normalized by the Euclidean length of all filters in the same block-row of $\mathbf{A}(\Theta)$, i.e., $\tilde{\theta}^{i,j} = \theta^{i,j} / \sqrt{\sum_{j=1}^{c_{\text{in}}} \sum_{k=1}^w \sum_{l=1}^w (\theta_{k,l}^{i,j})^2}$. Then $\rho(\mathbf{A}(\tilde{\Theta})^\top \mathbf{A}(\tilde{\Theta})) \leq w^2 c_{\text{out}}$

Proof. For $\mathbf{A} \in \mathbb{R}^{M \times N}$, each entry of the vector of row-squared-sums $\mathbf{v} \in \mathbb{R}^M$ is given by $\mathbf{v}_m = \sum_{n=1}^N \mathbf{A}_{m,n}^2$. Let $\mathbf{E} \in \mathbb{R}^{M \times N}$ with $\mathbf{E}_{m,n} = 1$ if $\mathbf{A}_{m,n} \neq 0$ and 0 otherwise. Then the eigenvalues of $\mathbf{A}^\top \mathbf{A}$ are bounded as $\rho(\mathbf{A}^\top \mathbf{A}) \leq \max(\mathbf{v}^\top \mathbf{E})$ [11, Prop. 4.1]. For a block matrix that is parameterized by convolutional kernels, $\mathbf{A}(\Theta)$, each row of each block contains all elements of the corresponding convolutional kernel. Normalizing each convolutional kernel by the Euclidean length of all kernels in the same block-row via $\tilde{\theta}^{i,j} = \theta^{i,j} / \sqrt{\sum_{j=1}^{c_{\text{in}}} \sum_{k=1}^w \sum_{l=1}^w (\theta_{k,l}^{i,j})^2}$, leads to $\mathbf{v}_m = 1$ for all rows. Thus, $\mathbf{v}^\top \mathbf{E}$ counts the number of nonzero entries in each column of $\mathbf{A}(\tilde{\Theta})$, where $\tilde{\Theta}$ indicates the normalized kernels. A matrix $\mathbf{A}(\Theta)$ where each block is Toeplitz, has the same number of nonzeros in every column if all convolutional kernels are of the same size, as we assumed. Every column in $\mathbf{A}(\tilde{\Theta})$ then contains w^2 nonzeros in each of the c_{out} blocks, so we obtained $\rho(\mathbf{A}(\tilde{\Theta})^\top \mathbf{A}(\tilde{\Theta})) \leq w^2 c_{\text{out}}$. \square

The above proposition provides a recipe to train CQnet with a certificate of nonexpansiveness, by normalizing the convolutional kernels according to Proposition 3.2, at each training iteration. This normalization together with a combination of the stability condition $\alpha_k \in (0, 2/\lambda_k]$ and the bound $\rho(\mathbf{A}(\tilde{\Theta})^\top \mathbf{A}(\tilde{\Theta})) \leq w^2 c_{\text{out}}$ tells us to select $\alpha_k \leq 2/(w^2 c_{\text{out}})$. The normalization corresponds to an ℓ_2 norm constraint on every set of convolutional kernels as organized in the block row of the matrix representation of all convolutional kernels. The normalization is then the projection as used in a stochastic projected gradient algorithm.

The bound and projection from Proposition 3.2 are in closed form, non-asymptotic, and computationally cheap (often $w \leq 7$ and c_{out} is a few dozen or few hundred per layer). While there is no claim that this bound is particularly tight, the computational simplicity is appealing, compared to some other conditions, for different network designs, that require iterative algorithms like Dykstra [54], Douglas-Rashford, [15], Bjorck Orthonormalization [59], or approaches that require training [60, 20] to achieve Lipschitz targets.

3.3 Illustrative example

To illustrate the intuitive and visually appealing operation of CQnet, consider a classification example of 1D data embedded in 2D (Figure 1). We classify by adding to the network’s last layer, output = $\mathbf{W} \mathbf{x}_f$, where \mathbf{W} is a learnable classifier matrix $\mathbf{W} \in \mathbb{R}^{\ell_{\text{class}} \times \ell_{\text{channels}}}$ and \mathbf{x}_f is the final state of the network. For simplicity, there is no constraint set C , all Q_k are half spaces as in the case of the ReLU activation, and the network has 20 layers with each $\alpha_k = 0.2$.

A trained neural network classifies the data (a point cloud) by transforming the data points into an organization that is linearly

separable. CQnet achieves this transformation of the data by moving each point toward the learned constraint sets. Figure 1 shows the data, network output, and final classification. We

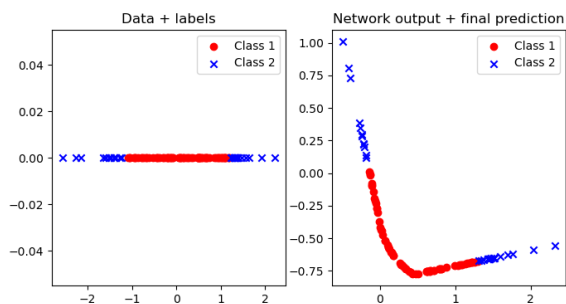


Figure 1: The 1D data are normally distributed numbers and assigned two classes. The network uses one additional dimension for this task. ‘Bending’ the data at the right spot is sufficient to achieve linear separability into the correct classifications.

are more interested in interpreting how the network arrived at the linearly separable representation. Simply plotting the trajectories of the data (Figure 2) provides a high-level overview, but we obtain more insight when we plot the trajectories along with the evolving constraint set and corresponding distance function that CQnet minimizes at every layer, see Figures 3 and 4. For this example, we see that the trajectories generally do not ‘catch up’ to the constraint sets. In a later section, we show how to enforce such behavior if desired. The figures show a convex-geometric description of the origins of the trajectories.

3.4 Training CQnet

Training CQnet is no different than many other neural networks. Given labels \mathbf{y} and a loss function $l(\mathbf{x}, \mathbf{y})$, training amounts to minimizing the loss between labels and network output

$$\min_{\{\mathbf{A}_k\}, \mathbf{W}} l(\mathbf{W}\mathbf{x}_f, \mathbf{y}) \text{ s.t.} \quad (10)$$

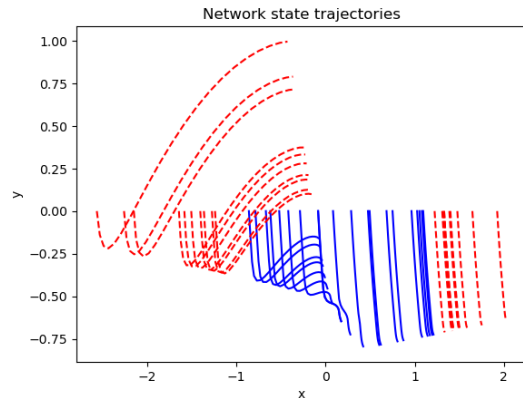
$$P_{C_k}(\mathbf{x}_k - \alpha_k \mathbf{A}_k^\top (\text{Id} - P_{Q_k}) \mathbf{A}_k \mathbf{x}_k) \\ \text{for } k = 1, 2, \dots, f-1 \text{ and } \mathbf{x}_1 = \mathbf{d}.$$

The matrix \mathbf{W} is a linear classifier. Practical minimization can proceed using automatic differentiation. It is implicit that the projection operators have a derivative defined almost everywhere. For instance, the derivative of the projector for bound constraints/ReLU at zero is set to 0, as in standard deep-learning software.

3.5 Including a bias term

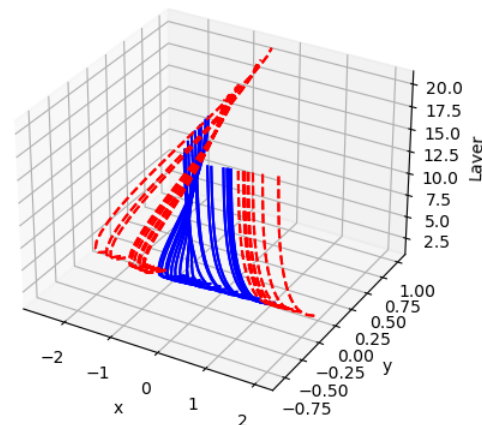
Many neural networks standardly incorporate a bias \mathbf{b} term via an affine transformation $\mathbf{A}\mathbf{x} + \mathbf{b}$. Adding a bias to CQnet is possible without even adjusting the form or notation by using the equivalence $\mathbf{A}\mathbf{x} + \mathbf{b} \leftrightarrow [\mathbf{A} \ \mathbf{b}] \begin{bmatrix} \mathbf{x} \\ 1 \end{bmatrix}$ and substituting it into (9) to obtain

$$\tilde{\mathbf{x}}_{k+1} = P_{\mathbf{x}_N=1}(\tilde{\mathbf{x}}_k - \alpha \tilde{\mathbf{A}}_k^\top (\text{Id} - P_{Q_k}) \tilde{\mathbf{A}}_k \tilde{\mathbf{x}}_k) \quad (11) \\ \text{for } k = 1, 2, \dots, f \text{ and } \tilde{\mathbf{x}}_1 = \begin{bmatrix} \mathbf{d} \\ 1 \end{bmatrix}$$



(a)

Network state trajectories 3D



(b)

Figure 2: The trajectories of the input data as viewed in a feature space and layer-feature space representation.

where $\tilde{\mathbf{A}} = [\mathbf{A} \ \mathbf{b}]$ and $\tilde{\mathbf{x}} = \begin{bmatrix} \mathbf{x} \\ 1 \end{bmatrix}$, and the projector $P_{\mathbf{x}_N=1}$ ensures the augmented last entry of $\tilde{\mathbf{x}}$ remains equal to one.

3.6 Optional energy conservation/normalization and state shifts

Two common building blocks for neural networks are normalizations of the state and energy conservation. The latter may arise from physics and control constraints. The former often includes shifting the state back to a mean of zero at each network layer.

The two above procedures also fit in CQnet via the projection P_C .

Energy conservation translates to the annulus constraint $\{\mathbf{x} \mid \sigma_1 \leq \|\mathbf{x}\|_2 \leq \sigma_2\}$, where σ_1 and σ_2 may be equal to the energy of the input data $\|\mathbf{d}\|_2$ or somewhat smaller/larger for approximate energy conservation. The projection is known in closed form, but because the set is not convex for $\sigma_1 > 0$, the projector is not nonexpansive, and stability is not guaranteed. If used for normalization only, ($\sigma_1 = 0, \sigma_2 > 0$) the set remains convex.

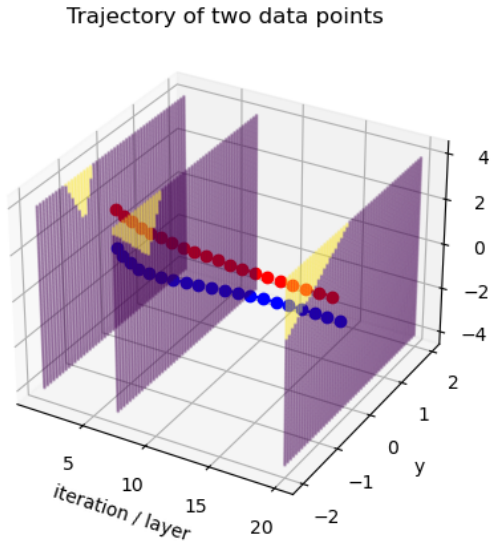


Figure 3: Trajectories for the trained CQnet corresponding to Figures 1 and 2, for one data point from two different classes. Constraint sets for three layers are also displayed.

Zero-mean states \mathbf{x}_k arise by shifting the mean to zero at each network layer. This shift is equivalent to projecting onto the orthogonal complement of the subspace spanned by the vector of all ones $\mathbf{e} = [1 \ 1 \ \dots \ 1]^\top$. Some basic linear algebra shows that this implies $C = \{\mathbf{x} \mid \mathbf{x} \in \text{col}(\mathbf{e})^\perp\} \leftrightarrow \{\mathbf{x} \mid \mathbf{x} \in \text{null}(\mathbf{e}^\top)\}$, so that the projection onto the set of vectors with zero mean is given by $P_C(\mathbf{x}) = (\mathbf{I} - P_{\text{col}(\mathbf{e})})\mathbf{x} = (\mathbf{I} - \mathbf{e}(\mathbf{e}^\top \mathbf{e})^{-1} \mathbf{e}^\top)\mathbf{x} \leftrightarrow P_C(\mathbf{x}) = \mathbf{x} - \mathbf{e} \frac{1}{n} \sum_{i=1}^n x_i$.

The examples section later on shows other uses for C related to optimal control.

3.7 Connection to networks as sequences of optimization problems

The interpretation of CQnet presented in the previous section helps us understand how the states propagate through the network. While the states in each layer track a changing constraint set in general, we can be more precise. For instance, by limiting the change in the matrices \mathbf{A}_k layer-by-layer. This restriction leads to a more gradually changing constraint set and allows the network states to ‘catch up’ to the constraint sets. A natural way to achieve this is to add regularization to the loss function that promotes slow variation between subsequent matrices \mathbf{A}_k and \mathbf{A}_{k+1} . Such regularization can also be found in training approaches for networks motivated by differential equations [10]. In our case, we emphasize that the smooth variation of the network weights is not a requirement for stability as shown in Theorem 3.1.

The network training (for a single example) with regularization applied to the weights of all f layers amounts to minimizing

$$\min_{\{\mathbf{A}_k\}} l(\mathbf{x}_f, \mathbf{y}) + \frac{\gamma}{2} \sum_{i=1}^{f-1} \|\mathbf{A}_{i+1} - \mathbf{A}_i\|_F^2 \quad \text{s.t.} \quad (12)$$

$$\mathbf{x}_{k+1} = P_{C_k}(\mathbf{x}_k - \alpha_k \mathbf{A}_k^\top (\text{Id} - P_{Q_k}) \mathbf{A}_k \mathbf{x}_k)$$

$$\text{for } k = 1, 2, \dots, f-1, \text{ and } \mathbf{x}_1 = \mathbf{d},$$

with penalty parameter $\gamma > 0$. Taking the slowly varying weights \mathbf{A}_k to the extreme leads to constant \mathbf{A}_k (weight sharing), such that the corresponding part of the network solves (approximately) the SFP $\mathbf{A}\mathbf{x} \in Q$ while $\mathbf{x} \in C$ (assuming all C_k and Q_k are fixed). Then, the full network consists of one or several intervals with constant parameters and is equivalent to solving a sequence of SFPs. Exploring this mode of operation of CQnet is left for future work, but it sets the stage to draw connections to prior work that recognizes some neural networks are equivalent to sequences of sparse-coding problems [61, 62], and methods that seek fixed points defined through non-explicit models like deep equilibrium models [63] or fixed point networks [17], differentiable optimization layers [64, 65] and other implicitly defined networks [66].

4 NUMERICAL EXAMPLES

The implementation and all examples are available at <http://...> Appendix A contains an additional example.

4.1 Multi-Agent control

CQnet naturally supports states that are always feasible w.r.t. a certain learned/not-learned constraint set while simultaneously approaching other constraint sets. The feasibility for these trajectory constraints holds by construction for training and inference. CQnet can thus solve some (optimal) control problems while simultaneously highlighting its geometrical interpretation.

Figure 5 introduces a discrete time and continuous space multi-agent path-finding problem, a version of which appeared in [67]. The task is simultaneously moving two agents from two possible starting areas to two targets.

The main challenges are moving through the corridor by avoiding the obstacles and staying at a safe distance from the obstacle while also not colliding with each other by preserving a safe inter-agent distance. The state vector $\mathbf{x} \in \mathbb{R}^4$ contains the coordinates of the two agents ($\mathbf{x}_a \in \mathbb{R}^2$ and $\mathbf{x}_b \in \mathbb{R}^2$). It is clear that any feasible trajectory should satisfy at least the state constraints

$$C \equiv \{\mathbf{x} \mid \|\mathbf{x}_a - \mathbf{x}_b\|_2 \geq 2.0\}, \quad \mathbf{x} = \begin{bmatrix} \mathbf{x}_a \\ \mathbf{x}_b \end{bmatrix} \quad (13)$$

$$Q_1 \equiv \{\mathbf{x} \mid \|\mathbf{x} - \mathbf{x}_{\text{target}}\|_2 \leq \epsilon\} \quad (14)$$

$$Q_2 \equiv \{\mathbf{x} \mid \|\mathbf{x} - \mathbf{x}_{\text{object},i}\|_2 \geq 1.0\} \forall \mathbf{x}_{\text{object},i} \quad (15)$$

where $\mathbf{x}_{\text{object},i}$ is one gridpoint of the object to avoid, and ϵ a small target tolerance. The nonconvex set C describes anti-collision between agents, Q_1 is a target constraint, and Q_2 is a nonconvex description of object avoidance.

Now consider an approach that combines ideas from neural ODEs, control, the CQnet, and the CQ algorithm. Below we state an optimal control approach to find trajectories for one or

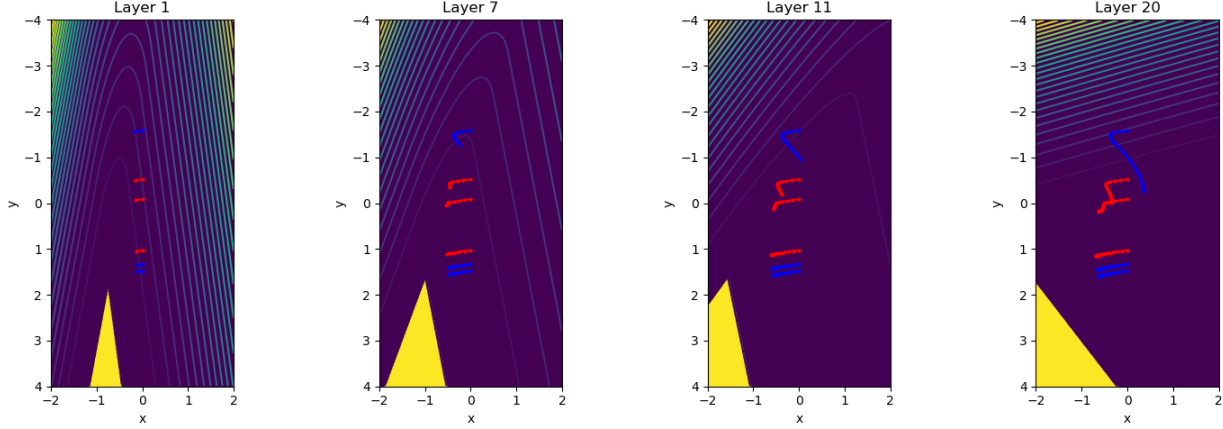


Figure 4: The constraint sets and corresponding squared-distance functions for a few layers of CQnet, and trajectories of a few input data.

a small set of non-adjustable initial conditions. It uses as the dynamics a mix of CQnet and the CQ algorithm for the above constraints,

$$\begin{aligned} \min_{\{\mathbf{A}_t\}} \quad & \beta_1 \sum_{t=1}^{t=T} J(\mathbf{x}_t, t) + \beta_2 \|\mathbf{x}_T - \mathbf{x}_{\text{target}}\|_2^2 \quad \text{s.t.} \quad (16) \\ \mathbf{x}_{t+1} = & P_C(\mathbf{x}_t - \sum_{i=1}^2 \alpha_i (\text{Id} - P_{Q_i}) \mathbf{x}_t \\ & + \alpha_3 \mathbf{A}_t^\top (\text{Id} - P_{Q_3}) \mathbf{A}_t \mathbf{x}_t) \quad \text{for } t \in \{1, T-1\} \\ \mathbf{x}_1 = & \mathbf{x}_{\text{start}} \end{aligned}$$

where P_{Q_3} is equivalent to the ReLU as in earlier examples. CQnet provides the dynamics with learnable weights $\mathbf{A}_t \in \mathbb{R}^{6 \times 4}$ for every layer, as well as contributions for the regular CQ iteration applied to the non-learnable constraints C , Q_1 , and Q_2 (see [68] for details related to the extension of the SFP to multiple constraint sets). The running costs for each time ($t = 1, \dots, T$) are $J(\mathbf{x}_t, t) = \|\mathbf{x}_{t+1} - \mathbf{x}_t\|$. The terminal cost appears as the constraint Q_1 and as a loss term.

CQnet creates states \mathbf{x}_t that are feasible with respect to the anti-collision constraints at every 'time-step' t , while simultaneously moving toward the target and away from the objects (if within the halo). Figure 5b illustrates that simply running the CQ algorithm (i.e., $\beta_1 = 0$ and $\alpha_3 = 0$) on a nonconvex problem can lead to agents that get stuck.

Learning via (16) does not use example trajectories or controls. The results with the neural network and running costs are shown in Figure 5c. Figure 5d displays multiple trajectories that show empirically that the agents can make it to the targets from any two starting positions from the initial training conditions. The experiment used a final time of $T = 100$.

For the nonconvex problem, it is also expected that some hyper-parameter tuning is required; we set $\beta_1 = 0.15$, $\beta_2 = 1$, $\alpha_1 = 0.1$, $\alpha_2 = 0.5$, and $\alpha_3 = 0.05$.

4.2 Fashion MNIST

While not the primary target application of CQnet, this example verifies that CQnet performs similarly to other networks on a simple general-purpose task: fashion-MNIST [69] classification. We compare against the Resnet [70], characterized by the layer $\mathbf{x}_{k+1} = \mathbf{x}_k - \alpha \text{ReLU}(\mathbf{A}_k \mathbf{x}_k + \mathbf{b}_k)$; and a variant with the symmetric layer [10] $\mathbf{x}_{k+1} = \mathbf{x}_k - \alpha \mathbf{A}_k^\top \text{ReLU}(\mathbf{A}_k \mathbf{x}_k + \mathbf{b}_k)$ that has more favorable stability properties. We compare these three networks because they have a superficially similar structure. Each network has seven layers with convolutional weight tensors, \mathbf{A}_k , of size $3 \times 3 \times 36 \times 36$ (36 channels) in all cases. There is a learnable opening/embedding layer of size $3 \times 3 \times 1 \times 36$, and a final classifier matrix that maps to the number of classes. Average poolings after layers two, four, and six reduce the feature size by a factor of two in each dimension. We look at a bare-bones comparison without data augmentation, no weight regularization, and training uses a fixed learning rate for stochastic gradient descent (batch size of one). The achieved test accuracy was CQnet: 90.91%, ResNet: 90.98%, and ResNet with symmetric layer: 90.89%, averaged over five training runs with different random initializations. So while it is encouraging that CQnet performs similarly, the primary reason for introducing CQnet is to offer a geometrical interpretation and employ it for satisfying trajectory constraints with provable stability properties.

5 CONCLUSIONS

This work introduces CQnet: a new neural network design with origins in the CQ algorithm for solving convex split-feasibility problems. The new network design provides novel set-based geometric insights into data points' trajectories when propagating through the network. The network also allows for incorporating multiple constraints on the trajectories that are satisfied at every layer while training and during inference. CQnet also gradually approaches another type of learnable constraint set via descent on its distance function. Because CQnet comprises projection operators and gradients of point-to-set distance functions, it naturally includes layer/state normalization, energy conservation, and certain non-linear activation functions. We provide a stability proof constructed from nonexpansive operators without

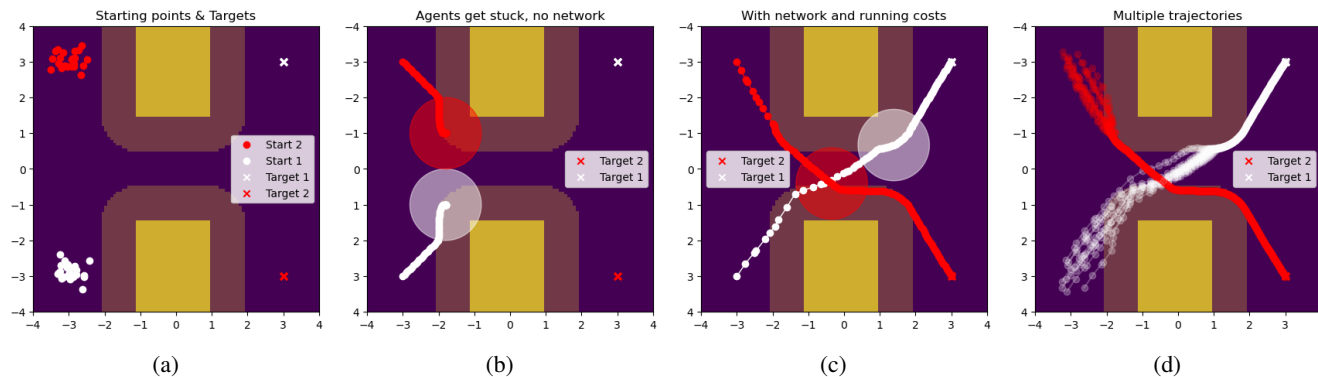


Figure 5: (a) Experimental setting with various possible starting locations, two targets, object (solid yellow), object safety halo (shaded). Agents need to stay a distance of 2.0 apart, which makes it impossible to simultaneously pass through the corridor. (b) Results of running the CQ algorithm (no network or learned parameters) with anti-collision constraints, target (ℓ_2 -ball) constraint, and object avoidance constraint (annulus constraint) as in (13). The agents can get stuck. (c) Results from CQnet with the constraints as in (13) and a time-dependent learned constraint that acts as the controller and dynamics. (d) Trajectories are shown for multiple initial conditions (still two agents at a time). All plots show trajectories at final time $T = 100$; radius= 1 circles in (b) and (c) are shown for $T = 60$.

simplifying assumptions on the variation of network weights per layer, the presence of the activation function, or layer normalization. Examples illustrate how CQnet provides a new convex-geometrical perspective on the internal operation of a neural network and how its constraint-handling capabilities connect it to problems with physical constraints and optimal control.

REFERENCES

- [1] William Huang and Richard P Lippmann. Neural net and traditional classifiers. In D. Anderson, editor, *Neural Information Processing Systems*, volume 0. American Institute of Physics, 1987. URL <https://proceedings.neurips.cc/paper/1987/file/4e732ced3463d06de0ca9a15b6153677-Paper.pdf>.
- [2] J. Makhoul, R. Schwartz, and A. El-Jaroudi. Classification capabilities of two-layer neural nets. In *International Conference on Acoustics, Speech, and Signal Processing*, pages 635–638 vol.1, 1989. doi: 10.1109/ICASSP.1989.266507.
- [3] Ewout van den Berg. Some insights into the geometry and training of neural networks. *arXiv preprint arXiv:1605.00329*, 2016.
- [4] Randall Balestriero, Romain Cosentino, Behnaam Aazhang, and Richard Baraniuk. The geometry of deep networks: Power diagram subdivision. In H. Wallach, H. Larochelle, A. Beygelzimer, F. d'Alché-Buc, E. Fox, and R. Garnett, editors, *Advances in Neural Information Processing Systems*, volume 32. Curran Associates, Inc., 2019. URL <https://proceedings.neurips.cc/paper/2019/file/0801b20e08c3242125d512808cd74302-Paper.pdf>.
- [5] Eldad Haber and Lars Ruthotto. Stable architectures for deep neural networks. *Inverse Problems*, 34(1):014004, dec 2017. doi: 10.1088/1361-6420/aa9a90.
- [6] E Weinan. A proposal on machine learning via dynamical systems. *Communications in Mathematics and Statistics*, 5(1):1–11, 2017.
- [7] Bo Chang, Lili Meng, Eldad Haber, Lars Ruthotto, David Begert, and Elliot Holtham. Reversible architectures for arbitrarily deep residual neural networks. In *AAAI Conference on AI*, 2018.
- [8] Yiping Lu, Aoxiao Zhong, Quanzheng Li, and Bin Dong. Beyond finite layer neural networks: Bridging deep architectures and numerical differential equations. In Jennifer Dy and Andreas Krause, editors, *Proceedings of the 35th International Conference on Machine Learning*, volume 80 of *Proceedings of Machine Learning Research*, pages 3276–3285. PMLR, 10–15 Jul 2018. URL <https://proceedings.mlr.press/v80/lu18d.html>.
- [9] Tian Qi Chen, Yulia Rubanova, Jesse Bettencourt, and David K Duvenaud. Neural ordinary differential equations. In S. Bengio, H. Wallach, H. Larochelle, K. Grauman, N. Cesa-Bianchi, and R. Garnett, editors, *Advances in Neural Information Processing Systems 31*, pages 6571–6583. Curran Associates, Inc., 2018. URL <http://papers.nips.cc/paper/7892-neural-ordinary-differential-equations.pdf>.
- [10] Lars Ruthotto and Eldad Haber. Deep neural networks motivated by partial differential equations. *Journal of Mathematical Imaging and Vision*, 62(3):352–364, 2020.
- [11] Charles Byrne. Iterative oblique projection onto convex sets and the split feasibility problem. *Inverse Problems*, 18(2):441–453, mar 2002. doi: 10.1088/0266-5611/18/2/310. URL <https://doi.org/10.1088%2F0266-5611%2F18%2F2%2F310>.
- [12] Patrick L Combettes and Jean-Christophe Pesquet. Deep neural network structures solving variational inequalities. *Set-Valued and Variational Analysis*, 28(3):491–518, 2020.
- [13] Patrick L. Combettes and Jean-Christophe Pesquet. Lipschitz certificates for layered network structures driven

- by averaged activation operators. *SIAM Journal on Mathematics of Data Science*, 2(2):529–557, 2020. doi: 10.1137/19M1272780. URL <https://doi.org/10.1137/19M1272780>.
- [14] Marzieh Hasannasab, Johannes Hertrich, Sebastian Neumayer, Gerlind Plonka, Simon Setzer, and Gabriele Steidl. Parseval proximal neural networks. *Journal of Fourier Analysis and Applications*, 26(4):1–31, 2020.
- [15] Matthieu Terris, Audrey Repetti, Jean-Christophe Pesquet, and Yves Wiaux. Building firmly nonexpansive convolutional neural networks. In *ICASSP 2020 - 2020 IEEE International Conference on Acoustics, Speech and Signal Processing (ICASSP)*, pages 8658–8662, 2020. doi: 10.1109/ICASSP40776.2020.9054731.
- [16] Ezra Winston and J. Zico Kolter. Monotone operator equilibrium networks. In H. Larochelle, M. Ranzato, R. Hadsell, M.F. Balcan, and H. Lin, editors, *Advances in Neural Information Processing Systems*, volume 33, pages 10718–10728. Curran Associates, Inc., 2020. URL <https://proceedings.neurips.cc/paper/2020/file/798d1c2813cbdf8bcdb388db0e32d496-Paper.pdf>.
- [17] Howard Heaton, Samy Wu Fung, Aviv Gibali, and Wotao Yin. Feasibility-based fixed point networks. *Fixed Point Theory and Algorithms for Sciences and Engineering*, 2021(1):1–19, 2021.
- [18] Christian Szegedy, Wojciech Zaremba, Ilya Sutskever, Joan Bruna, Dumitru Erhan, Ian J. Goodfellow, and Rob Fergus. Intriguing properties of neural networks. In Yoshua Bengio and Yann LeCun, editors, *2nd International Conference on Learning Representations, ICLR 2014, Banff, AB, Canada, April 14-16, 2014, Conference Track Proceedings*, 2014. URL <http://arxiv.org/abs/1312.6199>.
- [19] Mahyar Fazlyab, Alexander Robey, Hamed Hassani, Manfred Morari, and George Pappas. Efficient and accurate estimation of lipschitz constants for deep neural networks. In H. Wallach, H. Larochelle, A. Beygelzimer, F. d’Alché-Buc, E. Fox, and R. Garnett, editors, *Advances in Neural Information Processing Systems*, volume 32. Curran Associates, Inc., 2019. URL <https://proceedings.neurips.cc/paper/2019/file/95e1533eb1b20a9777749fb94fdb944-Paper.pdf>.
- [20] Yusuke Tsuzuku, Issei Sato, and Masashi Sugiyama. Lipschitz-margin training: Scalable certification of perturbation invariance for deep neural networks. In S. Bengio, H. Wallach, H. Larochelle, K. Grauman, N. Cesa-Bianchi, and R. Garnett, editors, *Advances in Neural Information Processing Systems*, volume 31. Curran Associates, Inc., 2018. URL <https://proceedings.neurips.cc/paper/2018/file/485843481a7edacbfce101ecb1e4d2a8-Paper.pdf>.
- [21] Zhouxing Shi, Yihan Wang, Huan Zhang, Zico Kolter, and Cho-Jui Hsieh. Efficiently computing local lipschitz constants of neural networks via bound propagation. *arXiv preprint arXiv:2210.07394*, 2022.
- [22] Gal Dalal, Krishnamurthy Dvijotham, Matej Vecerik, Todd Hester, Cosmin Paduraru, and Yuval Tassa. Safe exploration in continuous action spaces. *arXiv preprint arXiv:1801.08757*, 2018.
- [23] Yatin Nandwani, Abhishek Pathak, Mausam, and Parag Singla. A primal dual formulation for deep learning with constraints. In H. Wallach, H. Larochelle, A. Beygelzimer, F. d’Alché Buc, E. Fox, and R. Garnett, editors, *Advances in Neural Information Processing Systems* 32, pages 12157–12168. Curran Associates, Inc., 2019. URL <http://papers.nips.cc/paper/9385-a-primal-dual-formulation-for-deep-learning-with.pdf>.
- [24] Deepak Pathak, Philipp Krahenbuhl, and Trevor Darrell. Constrained convolutional neural networks for weakly supervised segmentation. In *The IEEE International Conference on Computer Vision (ICCV)*, December 2015.
- [25] George Papandreou, Liang-Chieh Chen, Kevin P. Murphy, and Alan L. Yuille. Weakly-and semi-supervised learning of a deep convolutional network for semantic image segmentation. In *Proceedings of the 2015 IEEE International Conference on Computer Vision (ICCV)*, ICCV 15, pages 1742–1750, USA, 2015. IEEE Computer Society. ISBN 9781467383912. doi: 10.1109/ICCV.2015.203. URL <https://doi.org/10.1109/ICCV.2015.203>.
- [26] Felix J Herrmann, Ali Siahkoohi, and Gabrio Rizzuti. Learned imaging with constraints and uncertainty quantification. *arXiv preprint arXiv:1909.06473*, 2019.
- [27] Hoel Kervadec, Jose Dolz, Meng Tang, Eric Granger, Yuri Boykov, and Ismail Ben Ayed. Constrained-cnn losses for weakly supervised segmentation. *Medical Image Analysis*, 54:88 – 99, 2019. ISSN 1361-8415. doi: <https://doi.org/10.1016/j.media.2019.02.009>.
- [28] Hoel Kervadec, Jose Dolz, Shanshan Wang, Eric Granger, and Ismail ben Ayed. Bounding boxes for weakly supervised segmentation: Global constraints get close to full supervision. In *Medical Imaging with Deep Learning*, 2020.
- [29] John Platt and Alan Barr. Constrained differential optimization. In D. Anderson, editor, *Neural Information Processing Systems*, volume 0. American Institute of Physics, 1987. URL <https://proceedings.neurips.cc/paper/1987/file/a87ff679a2f3e71d9181a67b7542122c-Paper.pdf>.
- [30] Pablo Márquez-Neila, Mathieu Salzmann, and Pascal Fua. Imposing hard constraints on deep networks: Promises and limitations. *arXiv preprint arXiv:1706.02025*, 2017.
- [31] Russell Stewart and Stefano Ermon. Label-free supervision of neural networks with physics and domain knowledge. In *Thirty-First AAAI Conference on Artificial Intelligence*, 2017.
- [32] Bas Peters. Point-to-set distance functions for output-constrained neural networks. *J. Appl. Numer. Optim.*, 4(2):175–201, 2022.
- [33] Mathis Brosowsky, Florian Keck, Olaf Dünkel, and Marius Zöllner. Sample-specific output constraints for neural networks. *Proceedings of the AAAI Conference on Artificial Intelligence*, 35(8):6812–6821, May 2021. doi: 10.1609/aaai.v35i8.16841. URL <https://ojs.aaai.org/index.php/AAAI/article/view/16841>.

- [34] Tue Boesen, Eldad Haber, and Uri M Ascher. Neural daes: Constrained neural networks. *arXiv preprint arXiv:2211.14302*, 2022.
- [35] Karol Gregor and Yann LeCun. Learning fast approximations of sparse coding. In *Proceedings of the 27th International Conference on International Conference on Machine Learning, ICML'10*, page 399–406, Madison, WI, USA, 2010. Omnipress. ISBN 9781605589077.
- [36] Suhas Lohit, Dehong Liu, Hassan Mansour, and Petros T. Boufounos. Unrolled projected gradient descent for multi-spectral image fusion. In *ICASSP 2019 - 2019 IEEE International Conference on Acoustics, Speech and Signal Processing (ICASSP)*, pages 7725–7729, 2019. doi: 10.1109/ICASSP.2019.8683124.
- [37] Vishal Monga, Yuelong Li, and Yonina C. Eldar. Algorithm unrolling: Interpretable, efficient deep learning for signal and image processing. *IEEE Signal Processing Magazine*, 38(2):18–44, 2021. doi: 10.1109/MSP.2020.3016905.
- [38] C Bertocchi, E Chouzenoux, M-C Corbineau, J-C Pesquet, and M Prato. Deep unfolding of a proximal interior point method for image restoration. *Inverse Problems*, 36(3):034005, feb 2020. doi: 10.1088/1361-6420/ab460a. URL <https://dx.doi.org/10.1088/1361-6420/ab460a>.
- [39] D. Youla. Generalized image restoration by the method of alternating orthogonal projections. *IEEE Transactions on Circuits and Systems*, 25(9):694–702, 1978. doi: 10.1109/TCS.1978.1084541.
- [40] Yair Censor and Tommy Elfving. A multiprojection algorithm using bregman projections in a product space. *Numerical Algorithms*, 8(2):221–239, 1994.
- [41] Jean-Baptiste Hiriart-Urruty and Claude Lemaréchal. *Fundamentals of convex analysis*. Springer Science & Business Media, 2012.
- [42] Charles Byrne. A unified treatment of some iterative algorithms in signal processing and image reconstruction. *Inverse Problems*, 20(1):103, nov 2003. doi: 10.1088/0266-5611/20/1/006. URL <https://dx.doi.org/10.1088/0266-5611/20/1/006>.
- [43] Yair Censor, Thomas Bortfeld, Benjamin Martin, and Alexei Trofimov. A unified approach for inversion problems in intensity-modulated radiation therapy. *Physics in Medicine & Biology*, 51(10):2353, apr 2006. doi: 10.1088/0031-9155/51/10/001. URL <https://dx.doi.org/10.1088/0031-9155/51/10/001>.
- [44] Mark Brooke, Yair Censor, and Aviv Gibali. Dynamic string-averaging cq-methods for the split feasibility problem with percentage violation constraints arising in radiation therapy treatment planning. *International Transactions in Operational Research*, n/a(n/a), 2019. doi: <https://doi.org/10.1111/itor.12929>. URL <https://onlinelibrary.wiley.com/doi/abs/10.1111/itor.12929>.
- [45] Genaro López, Victoria Martín-Márquez, Fenghui Wang, and Hong-Kun Xu. Solving the split feasibility problem without prior knowledge of matrix norms. *Inverse Problems*, 28(8):085004, jul 2012. doi: 10.1088/0266-5611/28/8/085004. URL <https://dx.doi.org/10.1088/0266-5611/28/8/085004>.
- [46] Aviv Gibali, Li-Wei Liu, and Yu-Chao Tang. Note on the modified relaxation cq algorithm for the split feasibility problem. *Optimization Letters*, 12(4):817–830, 2018.
- [47] Jinhua Wang, Yaohua Hu, Chong Li, and Jen-Chih Yao. Linear convergence of cq algorithms and applications in gene regulatory network inference. *Inverse Problems*, 33(5):055017, apr 2017. doi: 10.1088/1361-6420/aa6699. URL <https://dx.doi.org/10.1088/1361-6420/aa6699>.
- [48] Yekini Shehu and Aviv Gibali. New inertial relaxed method for solving split feasibilities. *Optimization Letters*, 15(6):2109–2126, 2021.
- [49] Patrick L. Combettes and Valérie R. Wajs. Signal recovery by proximal forward-backward splitting. *Multi-scale Modeling & Simulation*, 4(4):1168–1200, 2005. doi: 10.1137/050626090. URL <https://doi.org/10.1137/050626090>.
- [50] Mark Aleksandrovich Krasnosel'skii. Two comments on the method of successive approximations. *Usp. Math. Nauk*, 10:123–127, 1955.
- [51] W Robert Mann. Mean value methods in iteration. *Proceedings of the American Mathematical Society*, 4(3):506–510, 1953.
- [52] Ernest K. Ryu and Wotao Yin. *Large-Scale Convex Optimization: Algorithms & Analyses via Monotone Operators*. Cambridge University Press, 2022.
- [53] Ernest K Ryu and Stephen Boyd. Primer on monotone operator methods. *Appl. comput. math*, 15(1):3–43, 2016.
- [54] Hanie Sedghi, Vineet Gupta, and Philip M. Long. The singular values of convolutional layers. In *International Conference on Learning Representations*, 2019. URL <https://openreview.net/forum?id=rJevYoA9Fm>.
- [55] Andrzej Cegielski. Convergence of the projected surrogate constraints method for the linear split feasibility problems. *Journal of Convex Analysis*, 14(1):169–183, 2007.
- [56] Biao Qu and Naihua Xiu. A note on the cq algorithm for the split feasibility problem. *Inverse Problems*, 21(5):1655, sep 2005. doi: 10.1088/0266-5611/21/5/009. URL <https://dx.doi.org/10.1088/0266-5611/21/5/009>.
- [57] Qingzhi Yang. On variable-step relaxed projection algorithm for variational inequalities. *Journal of Mathematical Analysis and Applications*, 302(1):166–179, 2005. ISSN 0022-247X. doi: <https://doi.org/10.1016/j.jmaa.2004.07.048>. URL <https://www.sciencedirect.com/science/article/pii/S0022247X04006560>.
- [58] Fenghui Wang, Hong Kun Xu, and Meng Su. Choices of variable steps of the cq algorithm for the split feasibility problem. *Fixed Point Theory*, 12(2):489–496, 2011.
- [59] Cem Anil, James Lucas, and Roger Grosse. Sorting out Lipschitz function approximation. In Kamalika Chaudhuri and Ruslan Salakhutdinov, editors, *Proceedings of the 36th International Conference on Machine Learning*, volume 97 of *Proceedings of Machine Learning Research*, pages 291–301. PMLR, 09–15 Jun 2019. URL <https://proceedings.mlr.press/v97/anil19a.html>.

- [60] Moustapha Cisse, Piotr Bojanowski, Edouard Grave, Yann Dauphin, and Nicolas Usunier. Parseval networks: Improving robustness to adversarial examples. In Doina Precup and Yee Whye Teh, editors, *Proceedings of the 34th International Conference on Machine Learning*, volume 70 of *Proceedings of Machine Learning Research*, pages 854–863. PMLR, 06–11 Aug 2017. URL <https://proceedings.mlr.press/v70/cisse17a.html>.
- [61] Vardan Papyan, Yaniv Romano, and Michael Elad. Convolutional neural networks analyzed via convolutional sparse coding. *Journal of Machine Learning Research*, 18(83):1–52, 2017. URL <http://jmlr.org/papers/v18/16-505.html>.
- [62] Jeremias Sulam, Aviad Aberdam, Amir Beck, and Michael Elad. On multi-layer basis pursuit, efficient algorithms and convolutional neural networks. *IEEE Transactions on Pattern Analysis and Machine Intelligence*, 42(8):1968–1980, 2020. doi: 10.1109/TPAMI.2019.2904255.
- [63] Shaojie Bai, J. Zico Kolter, and Vladlen Koltun. Deep equilibrium models. In H. Wallach, H. Larochelle, A. Beygelzimer, F. d'Alché-Buc, E. Fox, and R. Garnett, editors, *Advances in Neural Information Processing Systems*, volume 32. Curran Associates, Inc., 2019. URL <https://proceedings.neurips.cc/paper/2019/file/01386bd6d8e091c2ab4c7c7de644d37b-Paper.pdf>.
- [64] Brandon Amos and J. Zico Kolter. OptNet: Differentiable optimization as a layer in neural networks. In Doina Precup and Yee Whye Teh, editors, *Proceedings of the 34th International Conference on Machine Learning*, volume 70 of *Proceedings of Machine Learning Research*, pages 136–145. PMLR, 06–11 Aug 2017. URL <https://proceedings.mlr.press/v70/amos17a.html>.
- [65] Akshay Agrawal, Brandon Amos, Shane Barratt, Stephen Boyd, Steven Diamond, and J. Zico Kolter. Differentiable convex optimization layers. In H. Wallach, H. Larochelle, A. Beygelzimer, F. d'Alché-Buc, E. Fox, and R. Garnett, editors, *Advances in Neural Information Processing Systems*, volume 32. Curran Associates, Inc., 2019. URL <https://proceedings.neurips.cc/paper/2019/file/9ce3c52fc54362e22053399d3181c638-Paper.pdf>.
- [66] Laurent El Ghaoui, Fangda Gu, Bertrand Travacca, Armin Askari, and Alicia Tsai. Implicit deep learning. *SIAM Journal on Mathematics of Data Science*, 3(3):930–958, 2021. doi: 10.1137/20M1358517. URL <https://doi.org/10.1137/20M1358517>.
- [67] Derek Onken, Levon Nurbekyan, Xingjian Li, Samy Wu Fung, Stanley Osher, and Lars Ruthotto. A neural network approach for high-dimensional optimal control applied to multiagent path finding. *IEEE Transactions on Control Systems Technology*, 31(1):235–251, 2023. doi: 10.1109/TCST.2022.3172872.
- [68] Yair Censor, Tommy Elfving, Nirit Kopf, and Thomas Bortfeld. The multiple-sets split feasibility problem and its applications for inverse problems. *Inverse Problems*, 21(6):2071–2084, nov 2005. doi: 10.1088/0266-5611/21/6/017. URL <https://doi.org/10.1088/0266-5611/21/6/017>.
- [69] Han Xiao, Kashif Rasul, and Roland Vollgraf. Fashion-mnist: a novel image dataset for benchmarking machine learning algorithms, 2017.
- [70] Kaiming He, Xiangyu Zhang, Shaoqing Ren, and Jian Sun. Deep residual learning for image recognition. In *Proceedings of the IEEE Conference on Computer Vision and Pattern Recognition*, pages 770–778, 2016.

A ILLUSTRATIVE 2D EXAMPLE.

Similar to the illustrative example of 1D data embedded in 2D as in section 3.3, we now show an example of 2D data embedded in 3D (Figure 6) and the effect of per-sample energy conservation. Training CQ net for the 100 data points $\mathbf{d}_i \in \mathbb{R}^3$ (where the third augmented dimension is always 0) proceeds by minimizing

$$\begin{aligned} \min_{\{\mathbf{A}_k\}, \mathbf{W}} l(\mathbf{W}\mathbf{x}_f, \mathbf{y}) \text{ s.t.} & \tag{17} \\ P_{C_k}(\mathbf{x}_k - \alpha_k \mathbf{A}_k^\top (\text{Id} - P_{Q_k}) \mathbf{A}_k \mathbf{x}_k) & \\ \text{for } k = 1, 2, \dots, f-1 \text{ and } \mathbf{x}_1 = \mathbf{d}. & \end{aligned}$$

For each data point \mathbf{d}_i we select all P_{C_k} as the annulus $C_k = \{\mathbf{x} \mid 0.9\|\mathbf{d}_i\|_2 \leq \|\mathbf{x}\|_2 \leq 1.1\|\mathbf{d}_i\|_2\}$ to guarantee approximate energy conservation. All P_{Q_k} are the halfspace (ReLU) constraint, all $\mathbf{A}_k \in \mathbb{R}^{3 \times 3}$, $\mathbf{W} \in \mathbb{R}^{1 \times 3}$, and the loss function $l(\mathbf{W}\mathbf{x}_f, \mathbf{y})$ is measured as binary cross-entropy.

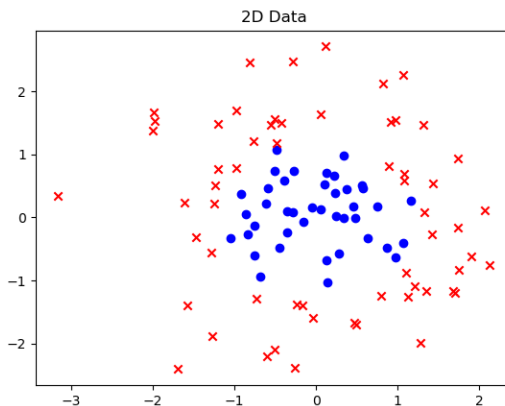


Figure 6: The 2D training data are normally distributed numbers and assigned two classes. The network uses one additional dimension for this task.

The predictions for all training and validation data is shown in Figures 7a and 7b, for CQnet with and without energy conservation. Figures 7c and 7d show the trajectories. The learned constraint sets are not shown because they are layer dependent and are a 4D quantity for this problem.

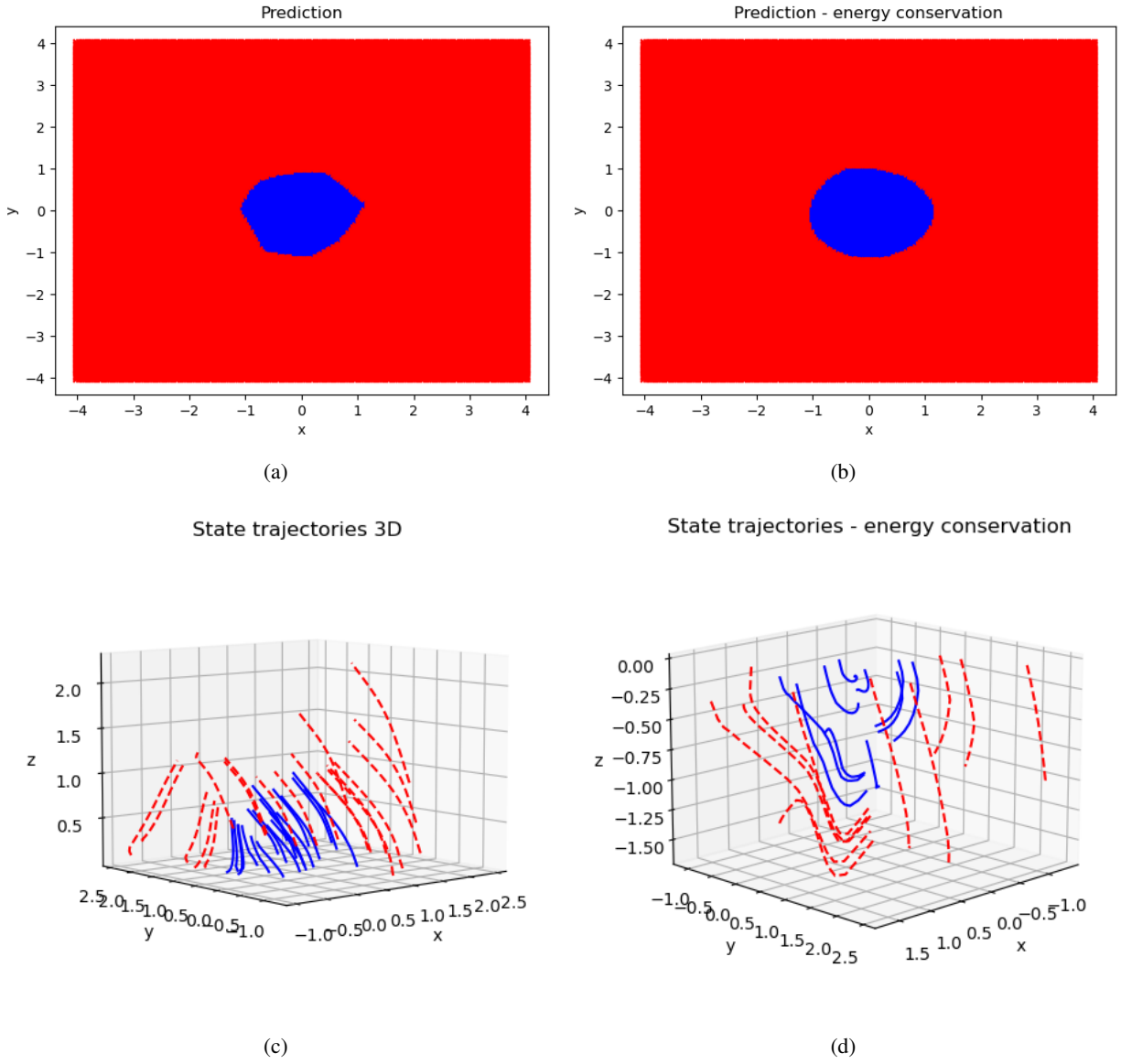


Figure 7: (a) & (b) Prediction on all training (Figure 6) and validation data. The additional energy constraints have a regularizing effect on this problem and increase the prediction accuracy. (c) & (d) Some trajectories for x-y-z at every layer in the CQnet, after training, for the data in Figure 6. While somewhat difficult to observe, the trajectories from CQnet with energy conservation are within the annulus.